STM JOURNALS

Journal of
Polymer & Composites

ISSN: 2321-2810 (Online)
ISSN: 2321-8525 (Print)
Volume 11, Special Issue 12, 2023
DOI (Journal): 10.37591/JoPC

http://engineeringjournals.stmjournals.in/index.php/JoPC/index

Research JoPC

Nanocrystalline Silver: Synthesis by High-Energy Ball Milling, X-ray Debye Temperature Analysis, and Diverse Applications

Purushotham Endla[1*], Endla Akhil Balaji[2]

Abstract

This research paper presents a comprehensive investigation into transforming micro-sized silver (Ag) powder into nanostructured Ag powder by applying high-energy ball milling. The ball milling process was executed over a total duration of 20 hours, with periodic sampling every 4 hours to monitor the evolving characteristics of the material. The particle size, lattice strain, Debye-Waller factor, and root mean square amplitudes of vibration were calculated by using X-ray powder diffraction techniques. Notably, a noteworthy observation emerged in this study: a discernible increase in the Debye-Waller factor was observed about lattice strain, indicating a previously unidentified correlation. The correlation between lattice strain and the influential Debye-Waller factor, this paper successfully estimated Debye-Waller. From the correlation between the strain and effective Debye-Waller factors have been estimated for Ag. The results of this research contribute to the fundamental understanding of the mechanical transformation of micro-sized Ag powder into nanostructured Ag powder and the implications for its physical properties.

Keywords: XRD, lattice strain, particle size, Debye-Waller factor, Debye temperature, applications.

INTRODUCTION

Chemists, physicists and materials scientists have shown great interest in the development of new methods for the synthesis of nanomaterials. The previous researchers [1–3] explained the characterization methods. Some other researchers [4–7] used various techniques. Additionally, biosynthesis and characterization of silver nanoparticles [8–10] using balloon flower plants, animal blood, and other methods have been explored for their preventive efficiency against bacterial species. A study by Singh et al. [11] focused on fabricating the parameters of silver nanoparticles (AgNPs) and assessing their antimicrobial activity. Quintero-Quiroz et al. [12] provided clear insights into the optimization of AgNPs, while S.A. Akintelu et al. [13] elucidated the antibacterial potency of AgNPs. Hasan et al. [14] discussed the environmental sustainability aspects of these nanoparticles. Xiaoyan et al. [15] and Geethika et al. [16] contributed to understanding green synthesis methods for AgNPs. Other researchers [17–19] have also explored various techniques for synthesizing AgNPs. Therefore, it is crucial to continue developing novel strategies for nanomaterial synthesis to advance this field further.

***Author for Correspondence**
Author Name: Purushotham Endla

[1]Associate Professor, Department of Physics, School of Sciences, SR University, Warangal, Telangana, India
[2]B.Tech Student, Computer Science and Engineering, Kakatiya Institute of Technology and Science, Hanamakonda, Telangana, India

Received Date: October 30, 2023
Accepted Date: December 12, 2023
Published Date: February 17, 2024

Citation: Purushotham Endla, Endla Akhil Balaji. Nanocrystalline Silver: Synthesis by High-Energy Ball Milling, X-ray Debye Temperature Analysis, and Diverse Applications. Journal of Polymer & Composites. 2023; 11(Special Issue 12): S140–S148.

Inagaki et al. [20, 21] calculated Debye-Waller factors by using X-Ray diffraction, Sirdeshmukh et al. [22] and Gopi Krishna et al. [23] studied the

effect of lattice strains on the Debye-Waller factors.

EXPERIMENTAL PROCEDURE

The paper you refer to describes an experimental study in which micro-sized Ag (silver) particles are transformed into nanostructured Ag NanoParticles [AgNPs] using a high-energy ball mill. The fundamental details and findings of the study can be summarized as follows.

- The study's primary goal is to reduce the particle size of Ag powder from the microscale to the nanoscale. Ball milling is the technique employed, carried out for a total duration of 20 hours.
- The sample is taken out at intervals of 4 hours during the milling process.
- The sample is characterized using X-ray powder diffraction, which provides information about the crystal structure and properties of the material.
- The particle size of the AgNPs is determined.
- The paper reports that in the case of Ag, the Debye-Waller factor increases as the lattice strain increases. This suggests a correlation between lattice strain and the Debye-Waller factor.
- Using the correlation between strain and the Debye-Waller factor, the study estimates the Debye-Waller factors for Ag at zero pressure. These values are crucial for understanding the thermal vibrations of atoms in the crystal lattice.
- This information can provide insights into the defects and properties of the nanosized Ag powder.

This work describes the successful transformation of micro-sized Ag powder into nanostructured Ag powder using high-energy ball milling. The findings suggest a relationship between lattice strain and the Debye-Waller factor and provide essential insights into the properties of nanosized AgNPs.

High Energy Ball Milling

Highly pure silver, sourced from the Solid State Physics Laboratory in New Delhi, served as the foundational material for this study. The methodology involved obtaining powder samples meticulously: the pure Ag metal ingots were delicately filed using a jeweler's file. A portion of this resulting powder was reserved for creating the initial piece. At the same time, the remainder underwent a transformative process in a high-energy planetary ball mill, specifically a Retsch PM 100 model from Germany. The milling process, conducted within a stainless steel chamber, introduced strains into the material and concurrently reduced the particle size. This mechanical alteration was achieved using tungsten carbide and zirconia balls, measuring 10 mm Φ and 3 mm Φ in diameter, respectively. The milling durations spanned 4, 8, 12, 16, and 20 hours, each imparting its unique impact on the material's characteristics. This carefully executed procedure laid the foundation for the subsequent investigations into the structural and mechanical properties of the silver powder, providing valuable insights into its evolution as a function of milling time.

X-Ray Diffraction Studies

In this study, X-ray diffractograms played a crucial role in analyzing the material's structural properties at various processing stages. X-ray diffractograms were acquired using a Philips CWU 3710 X-ray powder diffractometer, a reliable and widely utilized instrument for such investigations. The scans encompassed a 2θ range from 20 to 120 degrees, allowing for a comprehensive exploration of the material's crystallographic characteristics. Filtered CuKα radiation served as the X-ray source. This choice is common in X-ray diffraction (XRD) experiments due to its specific wavelength characteristics. The goniometer was set to operate at 0.5 degrees per minute, ensuring precise and controlled sample scanning. The chart speed was established at 20 mm per minute, generating precise and informative X-ray diffractograms. All XRD measurements were conducted under ambient room temperature conditions, maintaining a stable and consistent environment throughout the experiments. To enhance the accuracy of the data, observed integrated intensities underwent rigorous correction for thermal diffuse scattering. This correction step was carried out meticulously using the well-

established method developed by Chipman and Paskin [24]. This correction is crucial as it helps to eliminate artifacts and ensure the reliability of the obtained diffraction patterns.

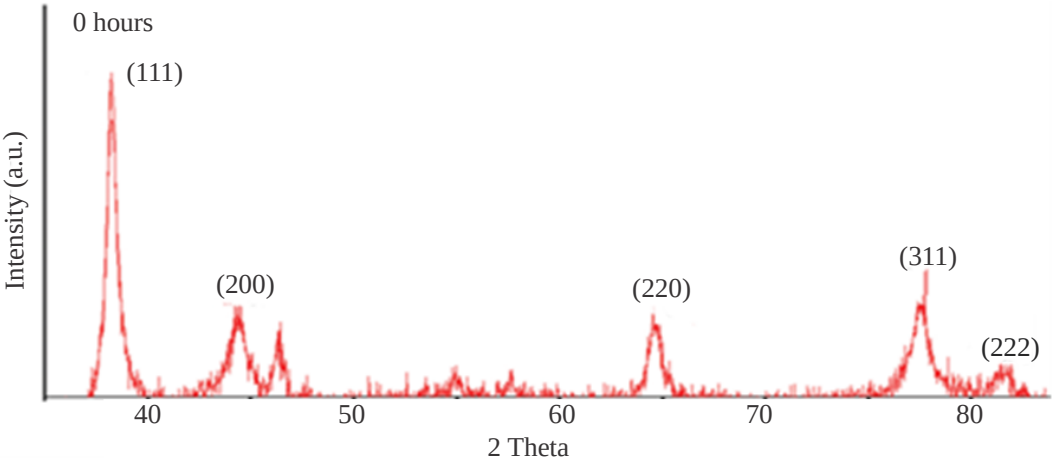

Figure 1. XRD patterns of AgNPs.

The XRD patterns of silver (Ag) are visually represented in Figure 1, capturing the evolution of the material's crystal structure throughout the milling process. These X-ray diffractograms are a fundamental tool for characterizing and comprehending the structural alterations induced by mechanical processing. They contribute valuable insights to the broader investigation, aiding in the understanding of the material's transformation under different milling durations and conditions.

ANALYSIS OF DATA

According to Klug and Alexander [25], Cromer and Waber [26], International Tables for X-ray Crystallography [27], and Cromer and Liberman [28], the observed intensity is given by

$$I_0 = I_c e^{-2B\left(\frac{\sin\theta}{\lambda}\right)^2} \quad (1)$$

where I_c is the intensity corresponding to the static lattice.

From Eq. (1) it can be seen that log (I_0/I_c) is linearly related to $(\sin\theta/\lambda)^2$. By a least square treatment of data, B was determined.

From the Debye-Waller theory

$$B = \left(\frac{8\pi^2}{3}\right)\langle u^2\rangle \quad (2)$$

where $\langle u^2\rangle$ is the mean-square amplitude of vibration.

$$B = \left(\frac{6h^2}{mk_BT}\right) W(x) \quad (3)$$

According to Benson and Gill [29], the function W(x) is given by

$$W(x) = \left[\frac{\phi(x)}{x^2} + \frac{1}{4x}\right] \quad (4)$$

where ø(x) is the Debye function and $x = \theta_M/T$, θ_M

From the above relation, the Debye temperature is given by

$$\theta_M = xT \quad (5)$$

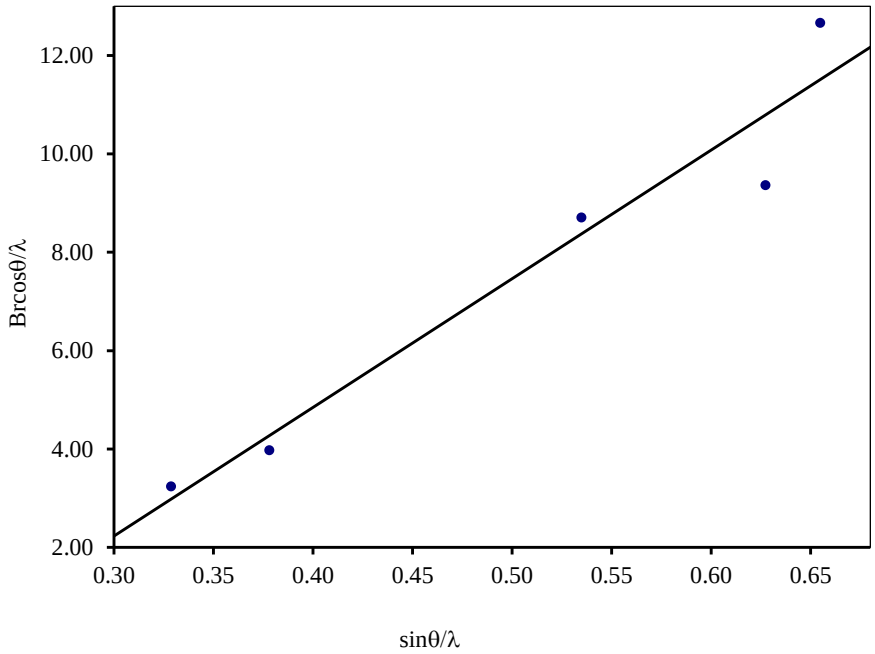

Figure 2. Plot of $B_r\cos\theta/\lambda$ Vs $\sin\theta/\lambda$ for Ag after milling for 12 hours.

The total peak broadening B_r may be expressed as,

$$B_r\cos\theta = \frac{k\lambda}{t} + \varepsilon \sin\theta \quad (6)$$

The lattice strains were determined from the plot of $B_r\cos\theta/\lambda$ against $\sin\theta/\lambda$ following standard procedures [30–37]. The Figure 2 $B_r\cos\theta/\lambda$ versus $\sin\theta/\lambda$ gives a straight line, the straight lineslope is equal to lattice strain and the intercept gives the particle size.

RESULTS AND DISCUSSION

In this study, the research findings regarding the values of AgNPs (Silver Nanoparticles) were compiled and presented in Table 1. The primary aim of this investigation was to explore the relationship between lattice strain (ε) and Debye-Waller factor (B) for AgNPs at various milling times, depicted in Figure 3. The Debye-Waller element of Ag powder samples exhibits sensitivity to lattice strain. In comparing the experimentally derived Debye-Waller factors with those calculated using lattice dynamical models, Vetelino et al. [38] observed disparities. These disparities were attributed to inaccuracies in the experimental values, primarily stemming from omitting thermal diffuse scattering (TDS) corrections. The iterative milling of the powder sample induces lattice distortion, resulting in the emergence of microstrains within the lattice structure, it becomes imperative to assess lattice strain when determining Debye-Waller factors from X-ray intensities of powder samples. In instances where lattice strain is substantial, it is prudent to apply a suitable correction, as exemplified in the present study.

Glyde [39] derived the following relation between the energy of vacancy formation (E_f) and the Debye temperature (θ) of a solid. The relation is

$$E_f = A(k/\hbar)^2 M\theta^2 a^2 \quad (5)$$

The validity of eq.(5) was verified for a number of fcc, bcc and hcp metals [40]. Therefore, the X-ray Debye temperatures obtained in the present work have been used to study the variation of vacancy formation energy as a function of lattice strain in Ag. The values of vacancy formation energies are also included in Table 1.

Table 1. The values of present investigation.

Metal	Milling time (hrs)	ε x 10^3	t(nm)	<u>(Å)	B(Å^2)	θ_M(K)	E_f(eV)
Ag	0	1.72	114	0.1595 (7)	0.67 (4)	219 (25)	1.81
	4	2.01	71	0.1710 (6)	0.77 (3)	204 (14)	1.57
	8	2.26	53	0.143 (7)	0.80 (4)	200 (16)	1.51
	12	3.24	46	0.1910 (7)	0.96 (3)	183 (12)	1.26
	16	3.72	36	0.1939 (6)	0.99 (3)	180 (8)	1.22
	20	4.06	28	0.1988 (7)	1.04 (4)	178 (11)	1.19

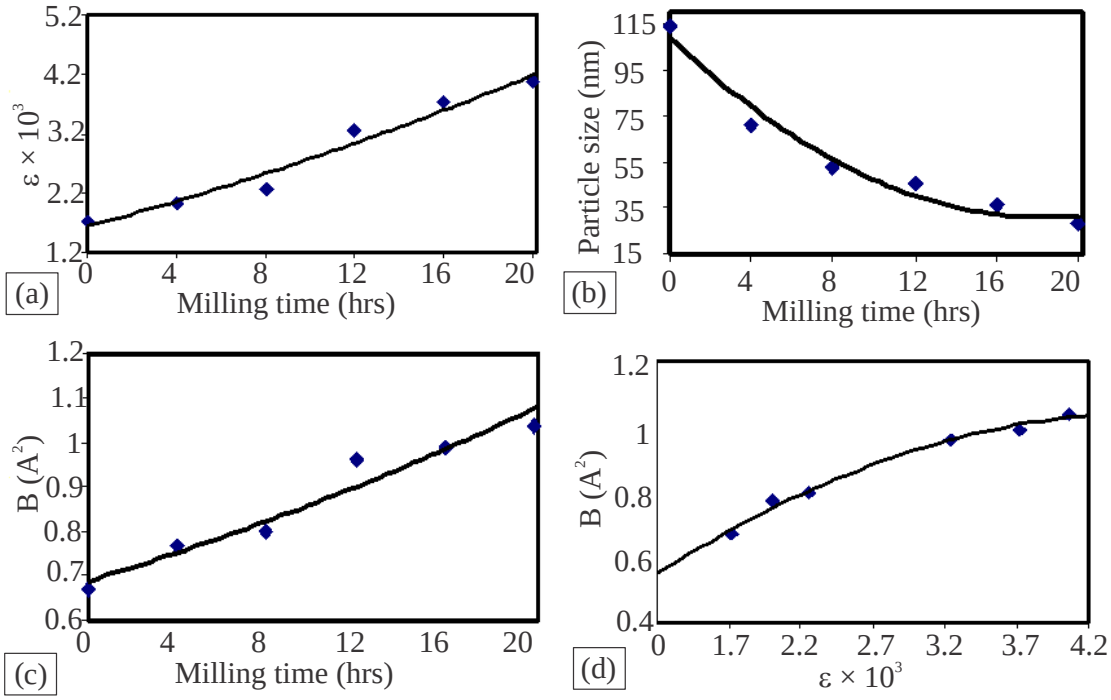

Figure 3. Plot of Milling time vs (a) lattice strain (b) Crystallite size, (c) Debye-Waller factor and (d) lattice strain Vs Debye-Waller factor curves for AgNPs.

From the table,

- Lattice strain increases as milling time increases. At 0 hours of milling, the strain is 1.72×10^{-3}, but it steadily rises to 4.06×10^{-3} after 20 hours. This indicates that the crystal lattice of the silver nanoparticles is becoming more distorted with prolonged milling.
- The lattice strain decreases from 114 nm at 0 hours to 28 nm at 20 hours, further confirming the distortion of the lattice structure with increased milling.
- Debye-Waller factor (DWF) increases as milling time increases. At 0 hours, DWF is 0.67 Å^2, but it increases to 1.04 Å^2 after 20 hours.
- The Debye temperature decreases with longer milling times. It starts at 219 K at 0 hours and decreases to 178 K at 20 hours.
- It drops from 1.81 eV at 0 hours to 1.19 eV at 20 hours. This decrease signifies that the lattice vibrations become less energetic with extended milling. These changes are indicative of the evolving structural and thermal characteristics of the material under the influence of mechanical milling.

From the Figure 3,

- As milling time increases, lattice strain increases, indicating a growing distortion of the crystal lattice structure.
- As milling time increases, the particle size decreases, reflecting the progressive reduction in the dimensions of the silver nanoparticles due to mechanical milling. This reduction occurs due to the mechanical forces exerted during milling, which break down larger particles into smaller ones over time.
- As milling time increases, the Debye-Waller factor also increases, signifying more excellent thermal vibrations and disorder within the material's crystal lattice.
- The increase in lattice strain is accompanied by a corresponding increase in the Debye-Waller factor, indicating a direct relationship between lattice distortion and enhanced thermal vibrations within the crystal lattice.

As lattice strain increases, the Debye-Waller factor also increases. This suggests that the lattice distortion and structural changes induced by milling lead to more pronounced thermal vibrations within the crystal lattice. This implies that the mechanical milling process effectively reduces the size of the AgNPs. The prolonged milling induces lattice strain, reducesparticle size, and enhances thermal vibrations, as evidenced by the increase in the Debye-Waller factor. These findings highlight the dynamic structural changes that occur during high-energy ball milling of silver nanoparticles.

Figure 4 the agreement between the particle sizes obtained from TEM (Transmission Electron Microscopy) images using the Hall Williamson method and those calculated by the ball milling method for zero and 20 hours is a significant finding in this study.

- *Zero Hours (Initial State):* When the material is in its initial state (zero hours of ball milling), the TEM analysis using the Hall Williamson method determined a particle size of 114 nm.
- *20 Hours (After Milling):* After 20 hours of ball milling, the TEM analysis, still using the Hall Williamson method, found that the particle size had reduced to 28 nm.
- Similarly, using the ball milling method, the particle size was calculated as 100 nm when the material was in its initial state (zero hours).
- *20 Hours (After Milling):* After 20 hours of ball milling, the particle size was calculated as 20 nm.

The critical observation here is that the TEM analysis using the Hall-Williamson method produced particle size estimates that closely match the results obtained from the ball milling method. Specifically, for the initial state (zero hours), both ways made values near 100–114 nm. Likewise, after 20 hours of Milling, both methods converged to indicate a reduction in particle size to around 20–28 nm.

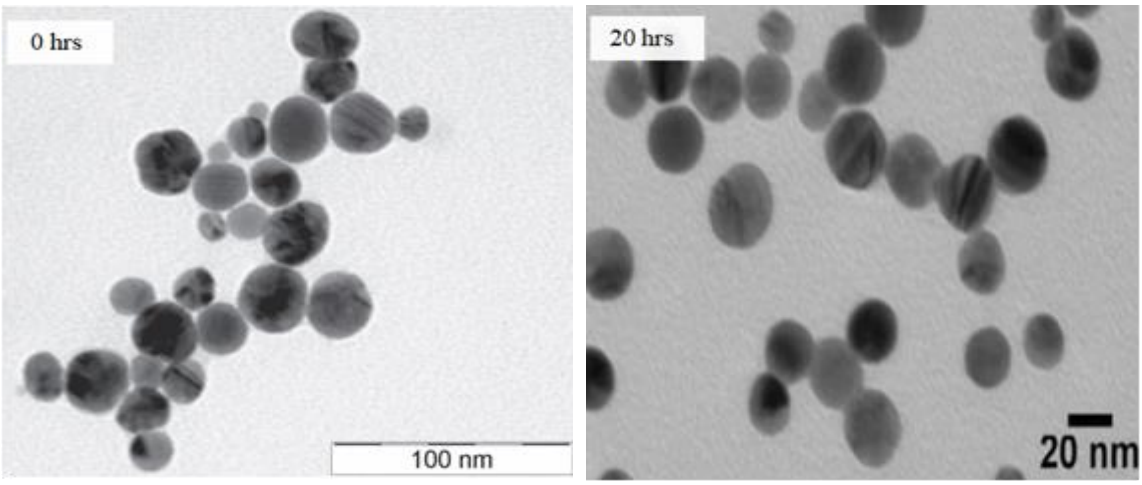

Figure 4. TEM images of AgNPs after ball milling time zero hours and 20 hours.

This agreement between the two independent measurement techniques strongly supports the accuracy and reliability of the reported particle size data. The Hall-Williamson method employed in TEM analysis provides consistent and corroborative results with the ball milling method, reinforcing the confidence in the findings and the validity of the experimental approach. The close agreement between particle size measurements obtained via TEM with the Hall Williamson method and the ball milling method for both the initial and milled states underscores the reliability and robustness of the particle size characterization in this study. It strengthens the scientific credibility of the reported results and provides a comprehensive view of the material's behavior during the high-energy ball milling process.

A few applications of AgNPs are given below:

- Nano-sized AgNPs can be incorporated into food packaging materials, benefiting from their antimicrobial properties to extend the shelf life of perishable goods.
- AgNPs can improve the efficiency of solar cells by enhancing light absorption and electron transport, influenced by their particle size and lattice strain.
- AgNPs' strong surface plasmon resonance, related to particle size, enhances the Raman scattering signal, making them valuable for sensitive chemical analysis.
- AgNPs' antimicrobial properties, driven by lattice strain, can be used in textiles to develop self-cleaning and odor-resistant fabrics.
- AgNPs can serve as contrast agents in medical imaging techniques like computed tomography (CT) and magnetic resonance imaging (MRI) due to their unique scattering properties, which relate to their particle size.

These applications highlight the versatility of silver nanoparticles in various fields, where their specific properties, influenced by the Debye-Waller factor, Debye temperature, lattice strain, and particle size, can be tailored to meet particular requirements.

CONCLUSIONS

- Milling silver (Ag) powders for 20 hours systematically affects particle size, resulting in a size reduction. This indicates that prolonged milling leads to a significant decrease in the size of the Ag particles.
- The milling process induces lattice strain in the material, suggesting that the crystal lattice structure of Ag is distorted and altered during milling.
- The influential Debye-Waller factor increases as a result of milling. This implies a greater degree of thermal vibration and disorder within the crystal lattice due to the mechanical milling.
- By extrapolating the relationship between the Debye-Waller factor and lattice strain, the zero strain Debye-Waller factor for Ag is determined.
- This value is vital for understanding the thermal vibrations of Ag atoms in the absence of lattice strain. The study explores how the energy of vacancy formation varies with lattice strain.
- This provides insights into the material's defect properties and energetics, shedding light on the impact of strain on vacancies in the crystal lattice. 20-hour milling of Ag powders reduces particle size, induces lattice strain, and increases the Debye-Waller factor.

The study also provides valuable data on the zero-strain Debye-Waller factor and the energy of vacancy formation, contributing to a comprehensive understanding of the material's behavior under mechanical strain.

REFERENCES

1. A. Singh, *et al.*Optimization of synthesis parameters of silver nanoparticles and its antimicrobial activity, Mater. Sci. Energy Technol., 3 (2020), pp. 232–236

2. J. Badmus, S. Oyemomi, O. Adedosu, *et al.* Photo-assisted bio-fabrication of silver nanoparticles using Annona muricata leaf extract: exploring the antioxidant, anti-diabetic, antimicrobial, and cytotoxic activities Heliyon, 6 (11) (2020), Article e05413
3. E.-Y. Ahn, Y. Park Anticancer prospects of silver nanoparticles green-synthesized by plant extracts, Mater. Sci. Eng. C, 116 (2020), Article 111253
4. S.A. Akintelu, Y. Bo, A.S. Folorunso, A review on synthesis, optimization, mechanism, characterization, and antibacterial application of silver nanoparticles synthesized from plants, J. Chem., 2020 (2020)
5. S.A. Akintelu, A.S. Folorunso, A.K. Oyebamiji, *et al.*, Antibacterial potency of silver nanoparticles synthesized using Boerhaaviadiffusa leaf extract as reductive and stabilizing agent, Int. J. Pharm. Sci. Res., 10 (12) (2019), pp. 374–380.
6. K. Hasan, M. Pervez, M. Talukder, *et al.* Community Entrepreneurship and environmental Sustainability of the Handloom sector, Handloom Sustainability and Culture, Springer, Singapore (2022), pp. 21–47
7. M.N. Pervez, M.Y. Hossain, M.E. Talukder, *et al.*, Nanomaterial-based smart and sustainable protective textiles, Protective Textiles from Natural Resources, Woodhead Publishing, Cambridge, United States (2022), pp. 75–111
8. P. Anbu, S.C. Gopinath, H.S. Yun, *et al.* Temperature-dependent green biosynthesis and characterization of silver nanoparticles using balloon flower plants and their antibacterial potential, J. Mol. Struct., 1177 (2019), pp. 302–309.
9. C. Tanase, L. Berta, A. Mare, *et al.* Biosynthesis of silver nanoparticles using aqueous bark extract of Picea abies L. and their antibacterial activity Eur. J. Wood Wood Prod., 78 (2) (2020), pp. 281–291
10. M.A. Kakakhel, F. Wu, H. Feng, *et al.* Biological synthesis of silver nanoparticles using animal blood, their preventive efficiency of bacterial species, and ecotoxicity in common carp fish Microsc. Res. Tech., 84 (8) (2021), pp. 1765–1774.
11. A. Singh, *et al.* Optimization of synthesis parameters of silver nanoparticles and its antimicrobial activity, Mater. Sci. Energy Technol., 3 (2020), pp. 232–236.
12. C. Quintero-Quiroz, N. Acevedo, J. Zapata-Giraldo, *et al.*, Optimization of silver nanoparticle synthesis by chemical reduction and evaluation of its antimicrobial and toxic activity, Biomater. Res., 23 (1) (2019), pp. 1–15.
13. S.A. Akintelu, A.S. Folorunso, A.K. Oyebamiji, *et al.*, Antibacterial potency of silver nanoparticles synthesized using Boerhaaviadiffusa leaf extract as reductive and stabilizing agent, Int. J. Pharm. Sci. Res., 10 (12) (2019), pp. 374–380.
14. K. Hasan, M. Pervez, M. Talukder, *et al.* Community Entrepreneurship and environmental Sustainability of the Handloom sector, Handloom Sustainability and Culture, Springer, Singapore (2022), pp. 21–47.
15. G. Xiaoyan, M. Sakil, Z. Xiaoming, *et al.*, One-pot green synthesis of Ag@AgCl nanoparticles with excellent photocatalytic performance, Surf Innov (2021), pp. 1–8.
16. B. Geethika, S. Sameer, L.A. Vishal, *et al.*Green synthesis of silver nanoparticles from heartwood extracts-Family of Fabaceae, Drug Invent. Today, 10 (3) (2018), pp. 3210–3213.
17. K. Hasan, P.G. Horváth, Z. Kòczán, *et al.*, Colorful and facile in situ nanosilver coating on sisal/cotton interwoven fabrics mediated from European larch heartwood, Scintific Reports, 11 (1) (2021), pp. 1–13
18. A. Menazea, Femtosecond laser ablation-assisted synthesis of silver nanoparticles in organic and inorganic liquids medium and their antibacterial efficiency, Radiat. Phys. Chem., 168 (2020), Article 108616
19. R. Mythili, T. Selvankumar, S. Kamala-Kannan, *et al.*, Utilization of market vegetable waste for silver nanoparticle synthesis and its antibacterial activity, Mater. Lett., 225 (2018), pp. 101–104
20. Inagaki, M. Furuhashi, H., T Ozeki *et al.*, *J Mater Sci*. 6, (1971) 1520.
21. Inagaki, M. Furuhashi, H. Ozeki, T and Naka, S. *J.Mater. Sci.* 8, (1973) 312.

22. Sirdeshmukh, D.B, Subhadra, K.G., Hussain, K.A., Gopi Krishna, N.,and Raghavendra Rao. B., *Cryst.Res.Technol*28, (1993) 15.
23. Gopi Krishna, N., and Sirdeshmukh., D.B., *Indian J Pure & Appl Phys*.31, (1993) 198.
24. Chipman, D.R., and Paskin, A., *J.Appl. Phys*.30, (1959) 1938.
25. Klug, H.P., and Alexander, L.E., (1974). *X-ray Diffraction Procedures* (John Wiley and Sons, U.S.A.).
26. Cromer, D.T., and Waber, J.T., *ActaCryst*. 18, (1965) 104.
27. International Tables for X-ray Crystallography (1968) Vol. III (Kynoch Press, Birmingham).
28. Cromer, D.T., and Liberman, D., *J. Chem. Phys*. 53, (1970) 1891.
29. Benson, G.C., and Gill, E.K., (1966) Table of Integral Functions Related to Debye-Waller factor, National Research Council of Canada, Ottawa.
30. Kaelble, E.F., *Handbook of X-rays* (New York Mc Graw ill) (1967)
31. Purushotham E, Gopi Krishna N (2010),Physica B (Elsevier): Condensed Matter, Volume 405, Issue 16, Pages, 3308–3311.
32. Purushotham E, Gopi Krishna N (2010), Indian Journal of Physics(springer), Volume 84, Issue 7, Pages, 887–893.
33. Purushotham E, Gopi Krishna N (2013), Bulletin of Materials Science (springer) Vol 36,Issue 6, Pages 973–976 (springer).
34. Purushotham E (2013),Journal of Engineering Science and Technology Review, Volume 6, Issue1, Pages, 83–86.
35. Purushotham E (2014), Bulletin of material science, (SCI, Springer), 37 (4), 773–778, www. Bull. Mater. Sci.
36. Purushotham E (2016), Journal of Nanoscience and Nanotechnology (SCI Journal), 2016, 16 No. 5(3), 2658–2662, doi:10.1166/jnn.2016.12462
37. Purushotham E (2020), IOP Conference Series: Materials Science and Engineering, 1757–8981, 2020, 981 022086, 1–6, doi:10.1088/1757-899X/981/2/022086
38. Vetelino, J.F., Gaur, S.P., Mitra, S.S., *Phys. Rev*.B5, (1972) 2360.
39. Glyde, H.R., *J.Phys and Chem Solids* (G.B) 28, (1967) 2061.
40. Micro-and Macro-Properties of Solids (Springer Series in Material Science) (2006)

